Effect of TiO_2 phase on the photocatalytic degradation of methylene blue dye

S.M. Tichapondwa*, J.P. Newman and O. Kubheka

Water Utilization Division, Department of Chemical Engineering, University of Pretoria, Pretoria, South Africa

*Corresponding author. shepherd.tichapondwa@up.ac.za

Highlights

- The TiO_2 phase greatly influences its photocatalytic activity towards Methylene blue dye.
- Dye decolourisation does not always translate to mineralisation of the organic pollutants.
- Copper doping increases the photocatalytic activity of TiO_2.

Abstract

Several industrial processes make use of dyes in order to impart colour into their products. These processes release large amounts of dye-containing wastewater which can be hazardous to human health and the environment. This has necessitated the development of cheap, reliable and sustainable technologies that can remediate the effluent, heterogeneous TiO_2 photocatalysis is one such technology that has proven successful. Different polymorphs of TiO_2 exist and literature suggests that the photocatalytic efficiency of various phases depends on the target pollutant. This study investigated the photocatalytic degradation of methylene blue (MB) dye using of three commercial TiO_2 powders with different crystal phases as catalysts. The materials properties for each catalyst were first determined using x-ray diffraction and microscopy. Degradation studies were then conducted on 10 ppm MB solutions using the three powders. Degussa P25 TiO_2, a mixture of anatase and rutile was the most efficient compared to the neat anatase and rutile powders, degrading 81.4% of the MB. This catalyst was chosen for optimisation studies, where 95% degradation was achieved at a 0.5 g/L catalyst loading and pH of 10. The degree of mineralisation decreased with increasing MB concentration. The effect of metal doping on the photocatalytic performance of the catalyst was also investigated. Copper doping increased degradation by 2% whilst zinc reduced it to 90%. The complete decolourisation of the MB coupled with the significant decrease in TOC upon completion of the degradation process, indicate that Degussa P25 catalysed photocatalysis is a viable pre-treatment technology in dye contaminated wastewater treatment.

Keywords: Photocatalysis; Methylene blue; Titanium dioxide; Metal doping

1. Introduction

The scarcity of fresh water sources is considered to be one of major challenges facing human civilization (Hoekstra et al., 2012). As such, concerted efforts are being made to develop strategies that maximize the usage of water that is already in circulation, one such strategy is water reuse (Salgot and Floch, 2018). This involves the immediate treatment of wastewater effluent to produce potable water. However, this strategy has been hampered by the inability of conventional biological wastewater treatment processes to remove a range of refractory organic pollutants thus negatively affecting the quality of the resultant water (Tichapondwa et al., 2018).

The textile industry is one of the largest consumers of water globally (Dilaver et al., 2018). The industry is also a leading anthropogenic contributor of organic and chemical pollutants found in wastewater with an average of 8000 chemicals being used during the production of textiles (Nimkar, 2018). These chemicals include acids, alkalis, dyes, hydrogen peroxide, starch, surfactants and dispersing agents (Holkar et al., 2016). Approximately 15% of all dyes used in the dyeing process are lost to the effluent (Houas et al., 2001). Once released, the dye coloured effluent may result in negative environmental effects such as the inhibition of photosynthesis and poisoning of aquatic life. The natural degradation products of these aromatic dyes tend to bioaccumulate resulting in detrimental health effects in humans. Methylene blue (MB), whose structure is shown in Fig. 1, is a low molecular weight, aromatic-based cationic dye (Imron et al., 2019). Its natural degradation products also consist of aromatic compounds and amines, which are highly carcinogenic and may result in histamine poisoning (Guidi and Gloria, 2012).

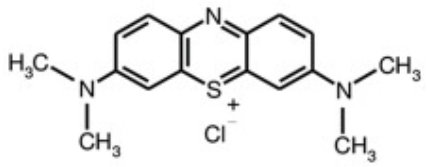

Fig. 1. Chemical structure of methylene blue dye.

Some of the common methods used to remediate organic pollutants such as MB and its degradation products include: adsorption, coagulation, membrane filtration and sedimentation. Whilst they have been shown to be efficient, these technologies all suffer in that the target pollutant is transferred from one medium to another and is not necessarily eliminated (Rauf et al., 2011). Secondary processes are therefore required in order to deal with the sludge or waste streams generated. The use of Advanced Oxidation Processes (AOP's) has been proposed as a potential solution. AOP's are driven by the generation of highly oxidizing free radicals which are capable of mineralizing organic compounds and therefore eliminating the formation of waste products (Daghrir et al., 2013).

Photocatalysis, is one of the AOP's that has received considerable attention due to its potential to being applied economically at a commercial scale. Titanium oxide (TiO_2) has been the photocatalyst of choice due to its low cost, chemical stability and high degradation efficiency when illuminated with UV light (Gil et al., 2017). There are three natural polymorphs of TiO_2, anatase, rutile and brookite. The first two are the most abundant and chemically stable phases and both occur in a tetragonal crystal habit. Brookite is less common and has an orthorhombic crystal structure. The differences in crystal structure and

particle morphology have been shown to influence the photocatalytic activity of semiconductor catalysts when applied to organic pollutant remediation (Ohtani et al., 2010). The current study evaluates the photocatalytic activity of anatase and rutile phase TiO_2 towards the degradation of MB dye in simulated wastewater. The performance of these catalysts was then related to key physical, chemical and photoelectric properties. Degussa P25 TiO_2, a commercial mixture of anatase and rutile was also investigated on its ability to degrade MB. The Degussa P25 TiO_2 has been specially engineered to reduce electron-hole recombination once the electron has been excited from the valence to the conduction band. This stabilisation results from the photoelectric interaction of the two phases upon UV light irradiation (Ohtani, 2008).

One of the major drawbacks associated with the use of TiO_2 photocatalysts is the high energy demand associated with UV light activation. This has led to concerted efforts in the development of photocatalysts with bandgap energies compatible with the energy of photons of visible light emitted by the sun (Wang et al., 2018). One strategy is the sensitization of TiO_2 through the introduction of doping agents on the catalyst surface (Gil et al., 2017). Studies have shown that incorporation of divalent transition metal ions into the TiO_2 lattice increases the photoelectric behaviour by creating an extra hole which acts as an accepter band close to that of the TiO_2 (Wattanawikkam and Pecharapa, 2015). This suppresses electron-hole recombination whilst shifting the catalyst to lower bandgap energies. The last part of the current study investigated the degradation of MB using TiO_2 doped with Cu and Zn.

2. Materials and methods

Methylene blue powdered dye was purchased from Inovia Hexachem. The anatase and rutile TiO_2 were purchased from Sigma-Aldrich whilst the Degussa P25 TiO_2 was obtained from Protea Specialty Chemicals. Copper (II) nitrate trihydrate, zinc (II) nitrate trihydrate and sodium hydroxide were also obtained from Sigma-Aldrich. Nitric acid (55%) was purchased from Glassworld.

2.1. Reactor setup

The batch reactor setup consisted of a 400 mL beaker placed on a magnetic stirrer. A 36 W Philips UV-C lamp was used as the light source. These items were enclosed in a 0.125 m^3 box lined with aluminium foil so as to eliminate the influence of external light. The 36 W UV lamp did not affect the temperature of the reactor, therefore no external cooling was required unlike similar setups previously described in literature (Mahlake et al., 2019).

2.2. Methods

The photocatalytic activity of the three different phases of TiO_2 was evaluated by following the degradation of 300 mL of a 10 ppm MB solution inoculated with 0.5 g/L of catalyst over a 100 min UV light irradiation period. The MB and catalyst suspension was stirred in the dark for 30 min in order to attain absorption-desorption equilibrium prior to irradiation. Approximately 5 mL of sample was collected at 20 min intervals. These sample aliquots were then centrifuged before determining the residual concentration using a WPA Light Wave II, Labotech UV–vis spectrophotometer. A standard calibration curve for the MB was determined prior to analyses. Control experiments with no irradiation (catalysis) and no catalyst (photolysis) were also carried out for the different TiO_2 catalysts. The efficiency of degradation was calculated using equation (1):

$$\% \text{ Degradation } = \frac{C_o - C}{C_o} \text{ x } 100 \quad (1)$$

Where C_0 is the initial concentration of phenol and C is the concentration of phenol at any given time, t.

Upon identifying the best performing TiO_2 catalyst, further experiments were conducted to establish the optimum parameters for the decolourisation of MB. These tests included varying the initial MB concentration as well determining the effect of varying pH. It should be noted that preliminary studies showed an optimal catalyst loading of 0.5 g/L, further addition of catalyst resulted in decreased degradation. This observation was attributed to shielding effect were if too many particles are present in water a lower fraction of the incident light is converted for electron excitation (Gnanaprakasam et al., 2015).

2.3. Catalyst modification

The best performing TiO_2 catalyst identified from the screening experiments was modified by introducing Zn and Cu metal dopants using a procedure similar to that described by Khuzwayo and Chirwa (2017). In this method, 1 g of TiO_2 was added to 50 mL of dopant solution with a concentration of 30 g/L. The resultant suspension was then sonicated for 30 min followed by 24 h of continuous agitation using a magnetic stirrer. The suspension was then centrifuged, washed with de-ionized water and oven dried at 110 °C for 6 h. After drying, the doped catalyst was calcined at a temperature of 500 °C for 2 h. The final product was then ground to a fine powder before use.

2.4. Characterization

Phase analysis of the different TiO_2 catalysts was carried out using a PANalytical X'Pert Pro powder x-ray diffractometer (XRD) in θ–θ configuration with an X'Celerator detector and variable divergence and fixed receiving slits with Fe filtered Co-Kα radiation (ʎ = 1.789 Å). The mineralogy was determined by selecting the best–fitting pattern from the ICSD database to the measured diffraction pattern, using X'Pert Highscore plus software. The elemental composition of the 3 TiO_2 catalysts was determined using an ARL Perform'X Sequential XRF instrument equipped with Quantas software for analysis. The morphology of the different powders was determined using a Zeiss Ultra PLUS 55 field emission scanning electron microscope (FESEM). The same instrument was used to analyse the elemental composition of the metal doped TiO_2 using the EDS/EDX attachment. A Jeol, JEM 1200X transmission electron microscope was used to further study the morphology of the individual catalyst particles. BET surface area measurements were acquired using a Micrometrics Tristar II instrument. Finally, the total organic carbon (TOC) and zeta potential measurements were determined using a Shimadzu TOC-V wp analyser and Malvern zetasizer Nano ZS, respectively. All samples were prepared using standard preparation methods for each of the characterization techniques.

3. Results and discussion

3.1. Catalyst characterization

X-ray diffraction analysis showed that both the anatase and rutile TiO2 powders were highly crystalline (Fig. 2). The Degussa P25 TiO2 powder was also highly crystalline and hd a

composition of 80.3% anatase and 19.7% rutile. This composition is consistent with literature, were the anatase to rutile ratio is reported to range between 70:30 and 80:20 (Ohtani et al., 2010). The variation in composition has been attributed to the lack of adequate methodologies to accurately determine the crystalline contents in nanometer-sized particles (Ohtani, 2008). It should be noted that higher photocatalytic behaviour has been reported in crystalline phases compared to the amorphous phase of the same compound (Kaur and Singh, 2012). This is due to easier transition of electrons from the valence to the conduction band of the semi-conductor material (Prasai et al., 2012). Since all three samples are highly crystalline, any variation in reactivity will most likely be a result of other material properties. A compositional analysis of the three powders was conducted using XRF and a breakdown of the main elements is shown in Table 1. The anatase and Degussa P25 were confirmed to be highly pure with minimal contamination. However, the rutile had a surprisingly high silicon content and low Ti composition. Since no silicon containing compounds were detected by XRD analysis, it was postulated that the silicon was present as amorphous SiO2. The rutile also had traces of several other metal elements and had the highest loss on ignition.

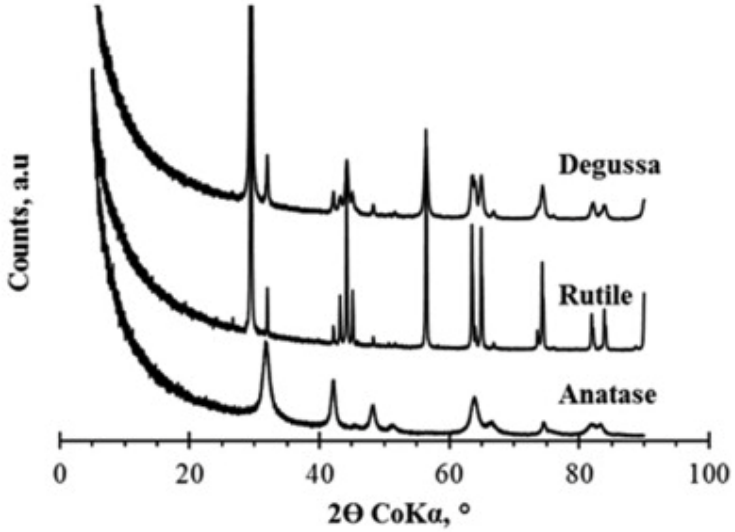

Fig. 2. X-ray diffraction spectra of the different TiO_2 phases.

Table 1. XRF results showing percentage main impurities in each TiO_2catalyst.

	Anatase	**Rutile**	**Degussa**
SiO_2	0.52	10.80	0.02
TiO_2	98.40	75.70	96.70
Na_2O	<0.01	1.44	<0.01
Cr_2O_3	<0.01	0.82	<0.01
Fe_2O_3	0.06	0.33	0.05
LOI[a]	0.86	3.19	9.97

[a]Loss on ignition when samples were roasted at 1000 °C.

The morphology of the particles is presented in Fig. 3. The SEM images showed that all the powders were highly agglomerated with small clumps made up of primary particles in the nano-range being observed. Transmission emission microscopy (TEM) was subsequently carried out in order to determine the nature of the primary particles. All the particles were shown to be less than 50 nm, however, the different TiO_2 phases had different morphologies. The anatase particles were near spherical, whilst the Degussa P25 particles were predominantly irregular and angular in shape. Rutile consisted of rod-like particles it sharp edges. The surface area of the particles is also directly influenced by their morphology. In the present study, rutile with rod-like morphology had the highest BET surface area (119.5 m^2/g) compared to 8.2 m^2/g for anatase and 56 m^2/g for the Degussa P25, respectively. Photocatalytic degradation is a surface reaction, therefore, high surface areas generally promote higher degradation since the pollutants adsorb faster onto the catalyst surface (Gnanaprakasam et al., 2015).

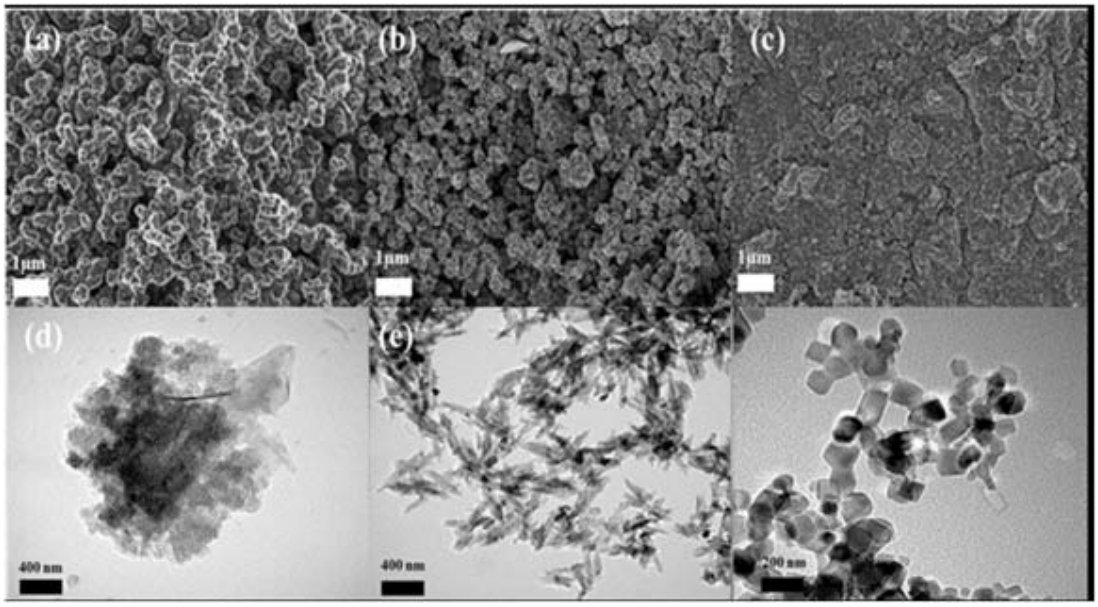

Fig. 3. (a)–(c) Scanning electron microscope (SEM) images for anatase, rutile and Degussa P25 TiO_2. (d)–(f) Transmission electron microscopy (TEM) images of for anatase, rutile and Degussa P25 TiO_2, respectively.

It has also been noted that particle morphology influences the photocatalytic activity of powders of the same composition due to the positioning/orientation of the valence and conduction bands. This in turn affects the quantum yield and electron-hole recombination rates (Wei et al., 2012). While it has generally been accepted that flower-like catalyst morphologies present the best photocatalysis properties due to their high surface areas and low electron-hole recombination rates (Sun et al., 2014). No strict photocatalytic activity hierarchy has been established for all the other particle morphologies. Besides the surface area and particle morphology, the degree of crystallinity, crystal orientation and band gap energy are regarded as most important factors in photocatalysis (Flores et al., 2014). Table 2 presents a summary of the material properties of the catalysts in the present study.

Table 2. Summary of material properties and photocatalytic activities of the catalysts used in the present study.

	Anatase	Rutile	Degussa P25
Material Properties			
BET surface area (m^2/g)	8.2	119.5	56.0
Morphology	Spherical	Rod/needle	Angular
TiO_2 Crystallinity	Crystalline	Crystalline mixed with amorphous SiO_2	Crystalline
Bandgap Energy (eV)	3.2[a]	3.0[a]	3.1[b]
MB Removal Mechanism			
Photolysis (%)	1.3	1.3	1.3
Adsorption (%)	4.2	30.1	7.4
Photocatalysis (%)	54.0	31.3	81.4

[a](Scanlon et al., 2013).
[b](Guayaquil-Sosa et al., 2017).

3.2. Photocatalytic activity of the different TiO_2 phases

The photocatalytic activity of the three TiO_2 catalysts was tested under uniform conditions. The first set of tests was a photolysis control experiment were 10 ppm of MB solution was irradiated with UV light in the absence of catalyst. Negligible decolourisation was observed after 100 min of irradiation (c.a 1.3%). The other control experiments investigated the adsorption properties of the catalysts in the absence of UV irradiation. Degussa P25 and anatase TiO_2 adsorbed 7.4% and 4.2% of the MB, respectively. This was much lower compared to the 30.1% recorded for rutile (Table 2). The high adsorption observed in rutile was attributed to its high surface area which allows for more adsorption sites compared to the other catalysts tested. It is worth noting that although rutile had a surface area double that of Degussa P25, it adsorbed 4 times more MB. It is postulated that the presence of the amorphous SiO_2 impurities which are known to possess excellent adsorption properties increased the adsorption capacity of rutile (Natarajan et al., 2018). The photocatalysis experiments revealed that Degussa P25 had superior photocatalytic properties resulting in 81.4% decolourisation compared to 54 and 31.3% for anatase and rutile, respectively. These results indicate that the rutile had virtually no photocatalytic activity since the adsorption and photocatalysis activity were almost similar. The higher decolourisation observed for Degussa P25 TiO_2 was consistent with observations from other studies on different pollutants (Hurum et al., 2003). It also confirms the stabilizing mechanism brought about by the interaction of the anatase and rutile crystallites in the Degussa P25. Fig. 4 shows that decolourisation was achieved faster by the Degussa TiO_2.

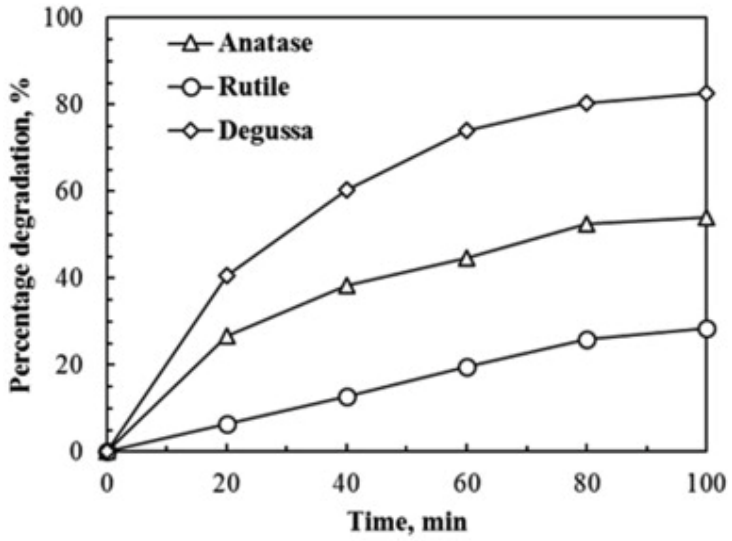

Fig. 4. Photocatalytic activity of the different TiO_2 catalysts on 10 mg/L MB contaminated water.

3.3. Effect of initial MB concentration

The effect of initial MB concentrations on the photocatalytic efficiency of the Degussa P25 was determined by varying concentration of MB while maintaining a catalyst loading of 500 mg/L. The solution with the lowest concentration (2.5 ppm MB) degraded the fastest and had the lowest residual concentration of MB (Fig. 5). Increase in MB concentration resulted in slower degradation and lower efficiency. A drastic decrease in efficiency was observed for the 15 ppm solution. It was postulated that the deep blue colour associated with this concentration resulted in decreased electron excitation in the catalyst since a significant portion of the UV light was adsorbed by the dark solution before reaching the catalyst. Similar trends have been reported by other researchers for textile dyes (Gnanaprakasam et al., 2015). While near complete degradation was observed for solutions with MB concentrations of 2.5–10 ppm, the extent of mineralisation was not as high for concentrations above 2.5 ppm (Fig. 6). The degree of mineralisation was determined by measuring the total organic carbon (TOC) before and after 100 min of UV irradiation. High TOC removal (86.9%) was attained for the 2.5 ppm MB solution. As the initial MB concentration increased, lower TOC removal percentages were obtained. Advanced oxidation processes in general and photocatalysis is particular are premised by their ability to completely mineralize organic compounds. Methylene blue dye ideally mineralizes according to the reaction shown in equation (2). The high MB degradation accompanied by low TOC removal observed for concentrations 5, 7.5 and 10 mg/L MB suggests that, though the MB structure is almost completely broken down through free radical oxidation, organic intermediate products are the dominant reaction products. Lin et al. (2018) reported the degradation pathway of MB and their gas chromatography – mass spectrophotometer data showed the presence of various smaller organic compounds compared to the initial MB molecule.

$$C_{16}HClN_3S + 25.5\,O2 \xrightarrow{TiO_2 + hv} HCl + H_2SO_4 + 3HNO_3 + 16CO_2 + 6H_2O \quad (2)$$

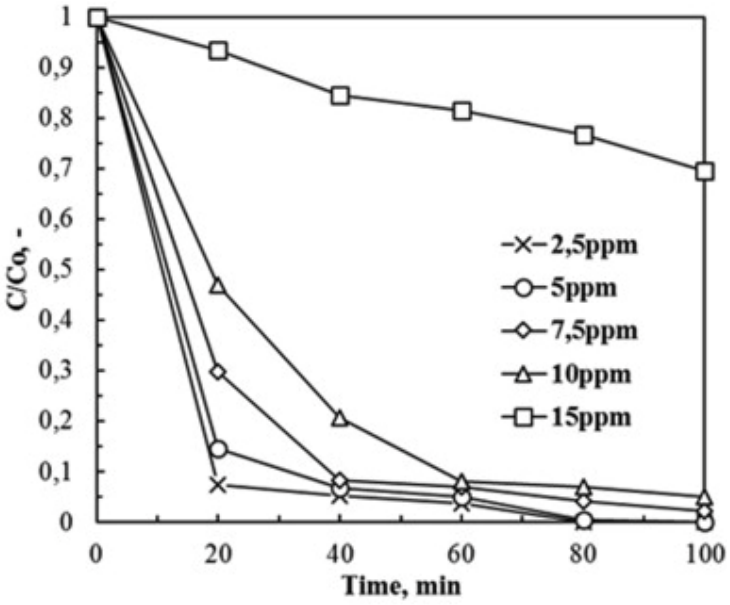

Fig. 5. Effect of initial MB concentration on the photocatalytic degradation efficiency of Degussa P25 TiO2.

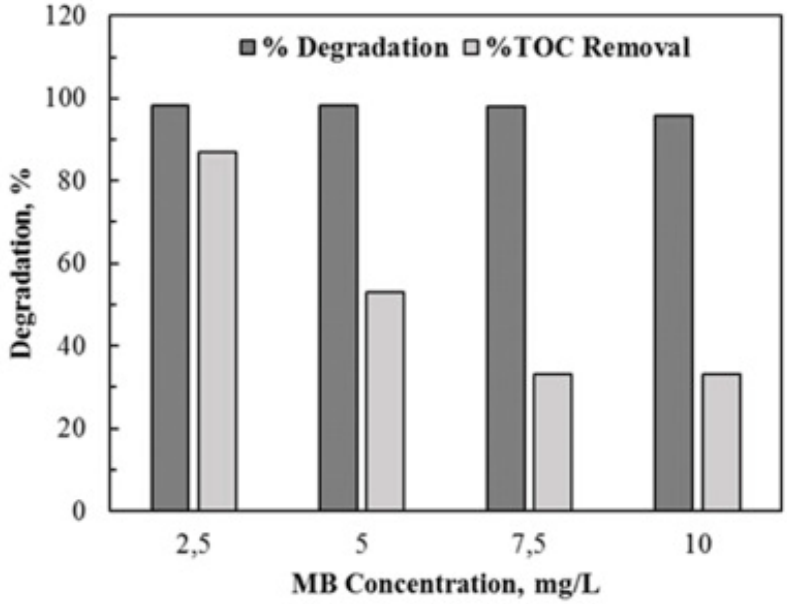

Fig. 6. Comparison between the degradation of MB and TOC removal after 100 min as a function of initial MB concentration.

3.4. Effect of pH

Fig. 7 shows the effect of initial solution pH on the photocatalytic degradation of 10 ppm of MB using Degussa P25 TiO_2 as a catalyst. The highest degradation was obtained at pH 11 with 93.4% of the MB being removed. The pH 7 MB solution had the next best degradation (84.4%) followed by pH 9, with the more acidic solutions achieving the least decolourisation. Photocatalytic reactions occur on the surface of the catalyst, therefore, the nature of the target

pollutant and its ease of adsorption onto the catalyst surface greatly impact the efficiency of the photodegradation process (Azeez et al., 2018). Colloidal particles by nature possess a net surface charge. Depending of the polarity of the target pollutant, adsorption can either be high due to the attraction of opposite charges, or it can be lowered by repulsion between identically charged pollutant and catalyst surface charges. The net surface charge of the catalyst is influenced by the pH of the medium in which it is suspended (Azeez et al., 2018). Fig. 8 presents the effect of solution pH on the zeta potential and hydrodynamic diameter (HDD) of the Degussa P25 particles in suspension. The zeta potential remained positive in the pH range 2–8 although the particle surface charge became less positive with increasing pH. In this pH range, the particles maintained an average HDD of 300 ± 80 nm, this suggests that a stable TiO_2 colloidal suspension was formed. The point of zero charge was observed at pH 9 and this was accompanied by a large increase in the hydrodynamic diameter (1400 nm). This showed that at pH 9, the suspension was destabilised and the primary particles formed agglomerates. When the pH was increased to 10 and above, the zeta potential dropped to negative values. This signified a negative net surface charge on the particles, which in turn resulted in stabilized suspensions with minimal agglomerate formation, as evidenced by a decrease in the HDD.

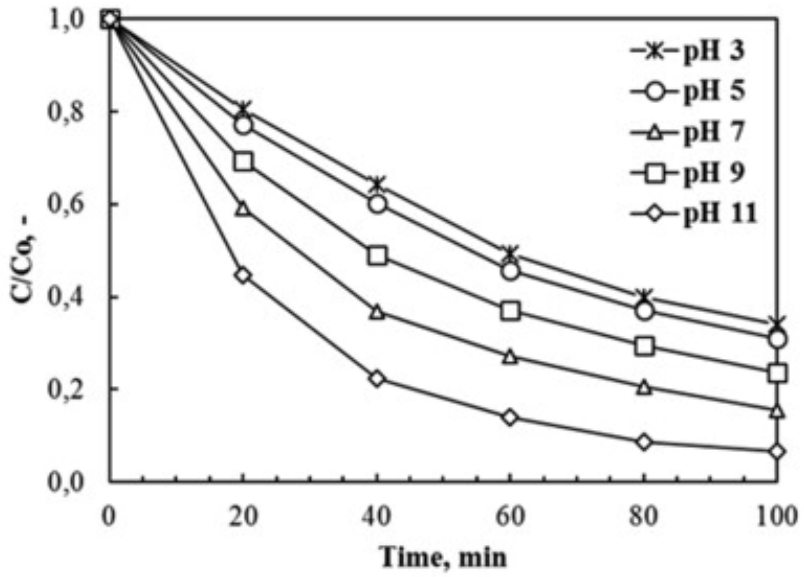

Fig. 7. Effect of solution pH on the photocatalytic degradation of MB.

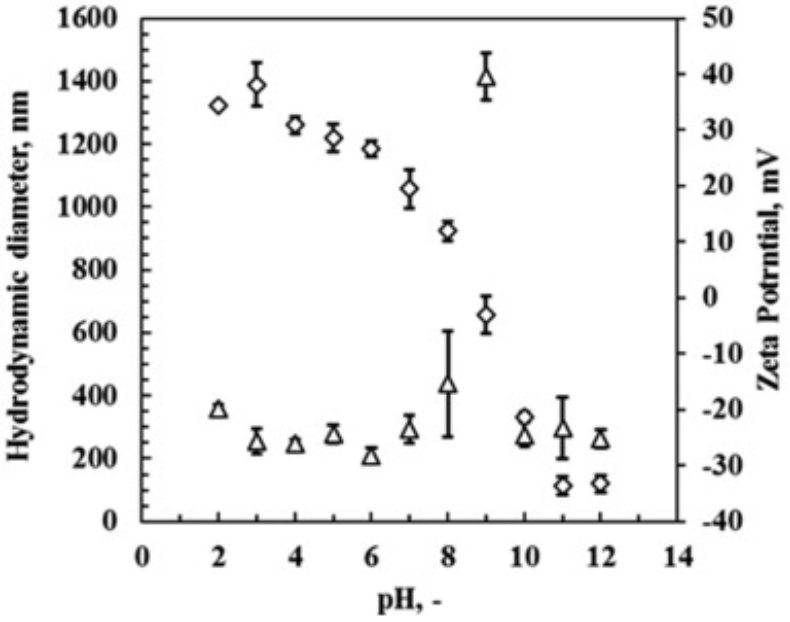

Fig. 8. Effect of pH on the zeta potential and hydrodynamic diameter (HDD) of the Degussa P25 TiO2.

These observations can be used to explain the results observed in Fig. 7. It should be noted that MB is a cationic dye, therefore, it has a positive net charge in solution (Fig. 1). At pH 10 and above, the catalyst has a negative zeta potential, this results in enhanced adsorption due to attraction between the opposite charges. The photocatalytic degradation is therefore improved as evidenced by the higher decolourisation obtained in this pH range. The opposite is true for the acidic pH, as repulsive forces between MB and catalyst dominate. The anomaly observed in the decolourisation trend at pH 9, was postulated to result from the agglomeration of the catalyst particles. Agglomeration reduced the active surface area available for reaction and also lowered the number of particles activated by UV irradiation resulting in decreased quantum yields.

3.5. Doping effects

Degussa P25 TiO_2 was modified by introducing copper and zinc as doping agents. The presence of these metals on the TiO_2 surface has been shown to improve degradation efficiency due to their ability to lower the band energy required for electron excitation (Daghrir et al., 2013). SEM-EDS analysis revealed that 1.24 wt% Cu and 0.24 wt% Zn were deposited on the TiO_2 surface upon completion of the doping process. Surprisingly, the copper-doped catalyst showed a slight increase in MB degradation (2%) whilst zinc doping reduced the degradation efficiency by 3%. The minimal change in reactivity of the catalyst after doping is likely due to the doping method being surface-based instead incorporating the doping agents into the crystal structure of the TiO_2. Fig. 9 shows that the photocatalysis reactions for all the catalysts followed a pseudo-first-order reaction which is described by equation (3)

$$\ln(C_o/C) = kt \quad (3)$$

Where C and C_o are the concentration at time t and initial concentration, and k is the apparent first-order rate constant. Degradation rates of 0.055 min^{-1}, 0.052 min^{-1} and 0.044 min^{-1} were obtained for the copper-doped, untreated and zinc-doped TiO_2, respectively.

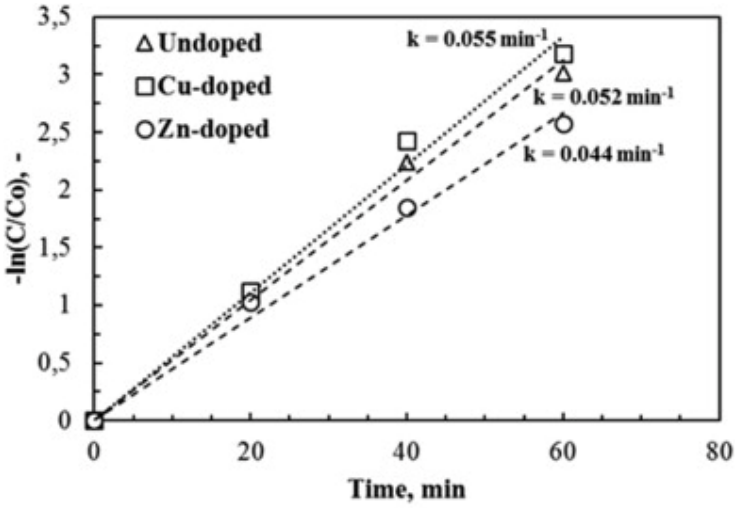

Fig. 9. Psuedo-first order kinetics for the degradation MB using undoped and metal-doped TiO_2.

4. Conclusion

The photocatalytic degradation of methylene blue dye using different forms of TiO_2 catalysts was investigated. Degussa P25, a mixture of anatase and rutile phase TiO_2 performed the best with 81.4% degradation being attained in 100 min of UV irradiation. The anatase TiO_2 degraded 54% of the MB whilst rutile attained 31.4% colour removal, which was attributed to adsorption rather than photocatalysis. pH had a significant effect on the decolourisation of MB with a maximum of 95.1 ± 0.1% being achieved under the following optimal conditions: catalyst loading of 0.5 g/L, initial pH of 11 and initial MB concentrations of 10 mg/L or lower. The degree of mineralisation was found to be significantly lower compared to MB degradation. This is attributed to the formation of organic intermediates. Modification of the catalyst through doping with copper increased the performance of the catalyst to 95.8 ± 0.4%, while zinc doping decreased the performance to 92.3 ± 1.8%. The modified and unmodified TiO_2 showed pseudo first order reaction kinetics. Based on the results observed for both MB decolourisation and the TOC removal, it can be concluded that UV light activated photocatalysis using Degussa P25 TiO_2 is a viable pre-treatment technology for the remediation of MB in water. It can be used to partially mineralize and breakdown the phenolic MB structure and produce organic intermediates that are bioavailable for biological degradation. This can also promote the wider use of water reuse in line with IWRM strategies.

Declaration of competing interest

The authors declare that they have no known competing financial interests or personal relationships that could have appeared to influence the work reported in this paper.

Acknowledgments

This work is based on the research supported in part by the National Research Foundation of South Africa (Grant Numbers: 117905) and the University of Pretoria's Research Development Programme (RDP).

References

Azeez, F., Al-Hetlani, E., Arafa, M., Abdelmonem, Y., Nazeer, A.A., Amin, M.O., Madkour, M., 2018. The effect of surface charge on photocatalytic degradation of methylene blue dye using chargeable titania nanoparticles. Sci..Rep. (U.K.) 8, 7104.

Daghrir, R., Drogui, P., Robert, D., 2013. Modified TiO2 for environmental photocatalytic applications: a review. Ind. Eng. Chem. Res. 52, 3581–3599.

Dilaver, M., Hocaoğlu, S.M., Soydemir, G., Dursun, M., Keskinler, B., Koyuncu, _I., Ağtas ¸ M., 2018. Hot wastewater recovery by using ceramic membrane ultrafiltration and its reusability in textile industry. J. Clean. Prod. 171, 220–233.

Flores, N.M., Pal, U., Galeazzi, R., Sandoval, A., 2014. Effects of morphology, surface area, and defect content on the photocatalytic dye degradation performance of ZnO nanostructures. RSC Adv. 4, 41099–41110.

Gil, A., García, A., Fernández, M., Vicente, M., González-Rodríguez, B., Rives, V., Korili, S., 2017. Effect of dopants on the structure of titanium oxide used as a photocatalyst for the removal of emergent contaminants. J. Ind. Eng. Chem. 53, 183–191.

Gnanaprakasam, A., Sivakumar, V., Thirumarimurugan, M., 2015. Influencing parameters in the photocatalytic degradation of organic effluent via nanometal oxide catalyst: a review. Indian J. Eng. Mater. Sci. 1–16, 2015.

Guayaquil-Sosa, J., Serrano-Rosales, B., Valadés-Pelayo, P., De Lasa, H., 2017. Photocatalytic hydrogen production using mesoporous TiO2 doped with Pt. Appl. Catal. B Environ. 211, 337–348.

Guidi, L.R., Gloria, M.B.A., 2012. Bioactive amines in soy sauce: validation of method, occurrence and potential health effects. Food Chem. 133, 323–328.

Hoekstra, A.Y., Mekonnen, M.M., Chapagain, A.K., Mathews, R.E., Richter, B.D., 2012. Global monthly water scarcity: blue water footprints versus blue water availability. PloS One 7, 1–9.

Holkar, C.R., Jadhav, A.J., Pinjari, D.V., Mahamuni, N.M., Pandit, A.B., 2016. A critical review on textile wastewater treatments: possible approaches. J. Environ. Manag. 182, 351–366.

Houas, A., Lachheb, H., Ksibi, M., Elaloui, E., Guillard, C., Herrmann, J.-M., 2001. Photocatalytic degradation pathway of methylene blue in water. Appl. Catal. B Environ. 31, 145–157.

Hurum, D.C., Agrios, A.G., Gray, K.A., Rajh, T., Thurnauer, M.C., 2003. Explaining the enhanced photocatalytic activity of Degussa P25 mixed-phase TiO2 using EPR. J. Phys. Chem. B 107, 4545–4549.

Imron, M.F., Kurniawan, S.B., Soegianto, A., Wahyudianto, F.E., 2019. Phytoremediation of methylene blue using duckweed (Lemna minor). Heliyon 5, e02206.

Kaur, K., Singh, C.V., 2012. Amorphous TiO2 as a photocatalyst for hydrogen production: a DFT study of structural and electronic properties. Energy Procedia 29, 291–299.

Khuzwayo, Z., Chirwa, E., 2017. The impact of alkali metal halide electron donor complexes in the photocatalytic degradation of pentachlorophenol. J. Hazard Mater. 321, 424–431.

Lin, J., Luo, Z., Liu, J., Li, P., 2018. Photocatalytic degradation of methylene blue in aqueous solution by using ZnO-SnO2 nanocomposites. Mater. Sci. Semicond. Process. 87, 24–31.

Mahlake, T., Tichapondwa, S.M., Tshuto, T.T., Chirwa, E.N.M., 2019. The effect of crystalline phase on the simultaneous degradation of phenol and reduction of chromium (VI) using UV/TiO2 photocatalysis. Chem. Eng. Trans. 76, 1279–1284.

Natarajan, S., Bajaj, H.C., Tayade, R.J., 2018. Recent advances based on the synergetic effect of adsorption for removal of dyes from waste water using photocatalytic process. J. Environ. Sci. 65, 201–222.

Nimkar, U., 2018. Sustainable chemistry: a solution to the textile industry in a developing world. Curr. Opin. Green Sustain. Chem. 9, 13–17.

Ohtani, B., 2008. Preparing articles on photocatalysis—beyond the illusions, misconceptions, and speculation. Chem. Lett. 37, 216–229.

Ohtani, B., Prieto-Mahaney, O., Li, D., Abe, R., 2010. What is Degussa (Evonik) P25? Crystalline composition analysis, reconstruction from isolated pure particles and photocatalytic activity test. J. Photochem. Photobiol., A 216, 179–182.

Prasai, B., Cai, B., Underwood, M.K., Lewis, J.P., Drabold, D., 2012. Properties of amorphous and crystalline titanium dioxide from first principles. J. Mater. Sci. 47, 7515–7521.

Rauf, M., Meetani, M., Hisaindee, S., 2011. An overview on the photocatalytic degradation of azo dyes in the presence of TiO2 doped with selective transition metals. Desalination 276, 13–27.

Salgot, M., Folch, M., 2018. Wastewater treatment and water reuse. Curr. Opin. Environ. Sci. Health 2, 64–74.

Scanlon, D.O., Dunnill, C.W., Buckeridge, J., Shevlin, S.A., Logsdail, A.J., Woodley, S.M., Catlow, C.R.A., Powell, M.J., Palgrave, R.G., Parkin, I.P., Watson, G.W., 2013. Band alignment of rutile and anatase TiO2. Nat. Mater. 12, 798–801.

Sun, D., Li, J., Feng, Z., He, L., Zhao, B., Wang, T., Li, R., Yin, S., Sato, T., 2014. Solvothermal synthesis of BiOCl flower-like hierarchical structures with high photocatalytic activity. Catal. Commun. 51, 1–4.

Tichapondwa, S.M., Tshemese, S., Mhike, W., 2018. Adsorption of phenol and chromium (vi) pollutants in wastewater using exfoliated graphite. Chem. Eng. Transact. 70, 847–852. https://doi.org/10.3303/CET1870142.

Wang, Y., Ganeshraja, A.S., Jin, C., Zhu, K., Wang, J., 2018. One-pot synthesis visible-light-active TiO2 photocatalysts at low temperature by peroxotitanium complex. J. Alloys Compd. 765, 551–559.

Wattanawikkam, C., Pecharapa, W., 2015. Synthesis and characterization of Zn-doped TiO2 nanoparticles via sonochemical method. Integrated Ferroelectrics Int. J. 165, 167–175.

Wei, J., Li, H., Mao, S., Zhang, C., Xu, Z., Dkhil, B., 2012. Effect of particle morphology on the photocatalytic activity of BiFeO3 microcrystallites. J. Mater. Sci. Mater. Electron. 23, 1869–1874.